

Cellulose Nanowhiskers Isolation and Properties from Acid Hydrolysis Combined with High Pressure Homogenization

Mingzhu Pan,* Xiaoyan Zhou, and Minzhi Chen

This study focused on cellulose nanowhiskers (CNWs) isolation using a combination of acid hydrolysis and high pressure homogenization, and investigated the effects of acid concentration (20, 40, and 60 wt%), hydrolysis temperature (20, 40, and 60 °C), and hydrolysis time (2, 4, and 6 h) on the geometry and chemical properties. After the combined treatment, nanoparticles were rodlike with a diameter of 11 to 33 nm, a length of 199 to 344 nm, and aspect ratio of 10 to 18, which are characteristic properties of CNWs. Fourier transform infrared spectroscopy (FTIR) and x-ray photoelectron spectroscopy (XPS) analyses showed that some breakages of intramolecular hydrogen bonds and glycosidic bonds occurred during the hydrolysis reaction of MCC. An increase in acid concentration from 20 to 60 wt% could effectively accelerate these breakages in cellulose molecules, leading to narrower, less polydisperse nanowhiskers with lower crystallinity.

Keywords: Cellulose nanowhiskers; High pressure homogenization; Acid hydrolysis; X-ray photoelectron spectroscopy (XPS)

Contact information: College of Wood Science and Technology, Nanjing Forestry University, Nanjing 210037, China, *Correspondence author: panmingzhu@yahoo.cn

INTRODUCTION

Nanocellulose has been used as reinforcements in biodegradable polymers in recent years because it is renewable, biodegradable, and chemically accessible, and because of its superior mechanical properties (Helbert *et al.* 1996; Samir *et al.* 2004; Oksman *et al.* 2006; Zhou *et al.* 2011). Incorporation of nanocellulose into a polymer matrix can significantly improve the mechanical property of composite materials at lower loading levels (Samir *et al.* 2005). It is expected that nanocellulose-based nanocomposites will open new areas for medicine, coating, packaging, electronics, adhesive, construction application, and others (Favier *et al.* 1995; Gray 2008; Kulkarni and Mahanwar 2011). Extensive studies have shown that nanocellulose derived from wood, agricultural crops and by-products, and bacterial cellulose can be obtained by chemical treatment, mechanical treatment, and enzymatic treatment (Oksman *et al.* 2009; Siró and Plackett 2010). Two different classes of nanosized cellulosic particles can be produced. The first one consists of nanocrystalline cellulose, and the second one is microfibrillated cellulose (Siqueira *et al.* 2010).

Acid hydrolysis of cellulose is a well-known chemical process, and it uses strong acids such as sulfuric acid and hydrochloric acid to remove the amorphous region. The process results in transverse cleavage of the nanofibril bundles, therefore breaking down the hierarchical structural into crystalline nanofibers or nanocrystalline cellulose (NCC), usually referred to as nanowhiskers (Martínez-Sanz *et al.* 2011). The morphology of the

obtained nanowhiskers using acid hydrolysis is influenced by acid-to-pulp ratio, the reaction time, temperature, and cellulose source. The nanowhiskers typically have a diameter of 2 to 20 nm, length of 100 to 600 nm, and aspect ratio of 10 to 100 (Beck-Candanedo *et al.* 2005; Siró and Plackett 2010). Dong *et al.* (1998) presented the preparation of colloid crystal of cellulose from microcrystalline cellulose (MCC). Bondeson *et al.* (2006) reported the effects of reaction conditions on the acid hydrolysis of cellulose using response surface methodology. They suggested that it was possible to obtain cellulose nanocrystals with a length between 200 and 400 nm and a width less than 10 nm with 63.5 wt% sulfuric acid in approximately 2 h. Elazzouzi-Hafraoui *et al.* (2008) studied the shape and size distribution of NCC resulting from the sulfuric acid hydrolysis of cellulose from cotton, MCC, and tunicate. Sadeghifar *et al.* (2011) reported NCC isolation using hydrobromic acid and surface characteristics with click reactions. However, these studies showed that NCC from acid hydrolysis has a wide range in size. Bai *et al.* (2009) explored a differential centrifugation technique for production of NCC with a narrow size distribution. Hamad and Hu (2010) investigated the relationship between sulfation and the degree of polymerization (DP) and ultrastructure as a function of NCC yield when a softwood kraft pulp was hydrolyzed using sulfuric acid. Li *et al.* (2011) prepared the NCC with diameter of 10 to 20 nm using the combined method of ultrasonication and acid hydrolysis from bleached softwood kraft pulp and reported that the ultrasonication could induce cellulose folding, surface erosion, and external fibrillation of pulp, resulting in the shorter length of 96 nm. Due to a low yield of 25 to 30% in NCC production, high yield NCC was also developed by sulfuric acid hydrolysis (Wang *et al.* 2012; Fan and Li 2012).

Another common method of nanocellulose isolation is high press shearing, and the resultant products are called microfibrillated cellulose (MFC). Such products typically have a length in excess of 1 μm , diameter of 10 to 40 nm, and aspect ratio of 100 to 150 (Siró and Plackett 2010). The manufacture of MFC is now generally performed by a mechanical treatment consisting of refining and a high pressure homogenizing process. Leitner *et al.* (2007) ran a suspension of sugar beet with a high-pressure homogenizer. During homogenization, the fibers were subjected to a large pressure drop with shearing and impact forces. This combination of forces promoted a high degree of microfibrillation of the cellulose fibers, resulting in the production of MFC. Liu *et al.* (2010) explored NCC suspension isolation from MCC using a combined acid hydrolysis and high pressure homogenization of 207 MPa. However, higher pressure would tend to increase the amount of energy used in potential industrial production.

So far, the separation of nanocellulose using acid hydrolysis and mechanical method has been studied extensively, but there is little information available on the effects of a combination of acid hydrolysis and high pressure homogenization on the morphology and other properties of nanocellulose. This study investigated the effects of the combined treatment on the surface morphology and size distribution, ultrastructure, and chemical properties of cellulose nanowhiskers.

EXPERIMENTAL

Raw Material and Preparation

MCC was supplied from Shanhe Pharmaceutical Excipients Co., Ltd. (Anhui, China). It is a white powder with no smell or taste, and it is insoluble in water, ethanol,

acetone, and toluene. Commercial sulfuric acid was used for acid treatment.

Cellulose Nanowhiskers Preparation

Cellulose nanowhiskers (CNWs) suspension was produced by following a procedure of acid hydrolysis and high pressure homogenization. Two grams of MCC powder were first placed in 100 mL aqueous solution of sulfuric acid with 20, 40, and 60 wt%. The mixtures were then stirred in a water bath, which was preheated to 20, 40, and 60 °C, and then kept for 2, 4, and 6 h (Table 1). Afterwards, the mixtures were washed with distilled water several times and centrifuged with a speed of 3500 rpm for 15 min (Anke TDL-40B, EHSY, China). The suspension was dialyzed with an ultrafiltration membrane until the pH of the suspension reached a constant value using a DDS-308A conductometer. The resultant suspension was then treated with a high pressure homogenizer (AH100D, ATS Engineering Inc). The pressure and cycle times was kept on 1200 bars and 8 respectively. The resultant suspensions were dried with a freeze-dryer (LGJ-10C, China) to obtain nanoparticles solid.

Table 1. Experimental Design of Cellulose Nanowhiskers Fractions

Conditions	H ₂ SO ₄ conc.	Hydrolysis time	Temperature
	wt%	h	°C
1	20	2	40
2	40	2	40
3	60	2	40
4	20	4	40
5	20	6	40
6	20	2	20
7	20	2	60

Surface Morphology

A Thermo company HITACHI S4800 cold field emission scanning electric microscope (FE-SEM) was used to observe the surface morphology of MCC and freeze-dried nanoparticles. The samples were coated with gold before examination. The morphology of nanoparticle suspension was examined using transmission electron microscopy (TEM, JEM-2100, JEOL) at 120 kV. A drop of nanoparticle suspension was placed on a copper grid and dried at room temperature (25 °C). Size distribution of nanoparticles from the TEM images were measured with Imaging MVS3000 software, and 500 counts were taken for each sample.

XPS Analysis

X-ray photoelectron spectroscopy (XPS) analyses were performed to determine the chemical composition of cellulose nanowhiskers. A small quantity of sample was mounted on double-sided adhesive tape and placed in a PHI5000 VersaProbe spectrometer (ULVAC-PHI, Japan) with a hemispherical energy analyser, using a monochromatic Al/K source (1486.6 eV). Spectra were analysed using the XPSPEAK41 software. A Shirley 'baseline' was used for background subtraction, whereas Gaussian (80%)-Lorentzian (20%) peaks were used for spectral deconvolution.

FTIR Spectroscopy

Fourier transform infrared (FTIR) spectra of MCC and CNWs from the treatments were obtained using a FTIR 360 (Thermo Nicolet). Samples and KBr powder (1:60) were uniformly ground and pressed to form pellets. All sample spectra were recorded in the 4000 to 400 cm^{-1} range with a resolution of 0.5 cm^{-1} . Thirty two scans were carried out for each spectrum. Two replicated measurements were carried out for each sample.

WAXD Investigation

Wide angle X-ray diffraction (WAXD) was performed to investigate the ultra-structure of the CNWs affected by treatments. A small quantity of sample was mounted on double-sided cello tape and placed in a DX-2000 diffractometer with a Cu anode, operating at 40 kV and 30 mA. The crystallinity index of the CNWs was calculated according to Eq. (1),

$$CrI = \frac{I_{(002)} - I_{(am)}}{I_{(002)}} \times 100 \quad (1)$$

where, I_{002} is the counter reading at peak intensity at a 2θ close to 22° , and I_{am} is the amorphous counter reading at a 2θ close to 18° (Hamad and Hu 2010).

RESULTS AND DISCUSSION

Effects of Treatment on Morphology

Figure 1 shows a FE-SEM micrograph of MCC, which consisted generally of stiff, rod-like particles with a width of 15 to 20 μm and length of 40 to 60 μm . MCC is a naturally occurring substance that is obtained at an industrial scale through hydrolysis of wood and cotton cellulose using dilute mineral acids (El-Sakhawy and Hassan 2007).

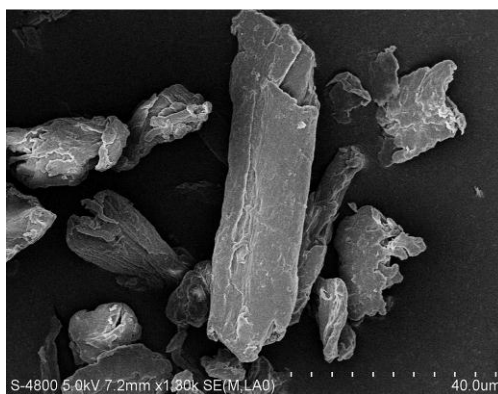
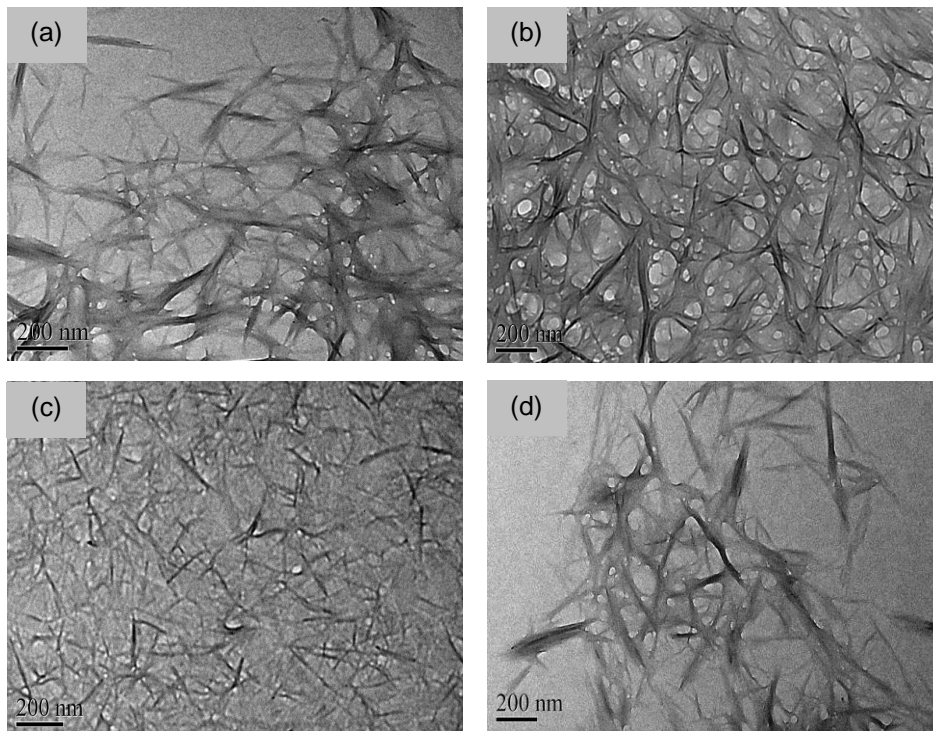
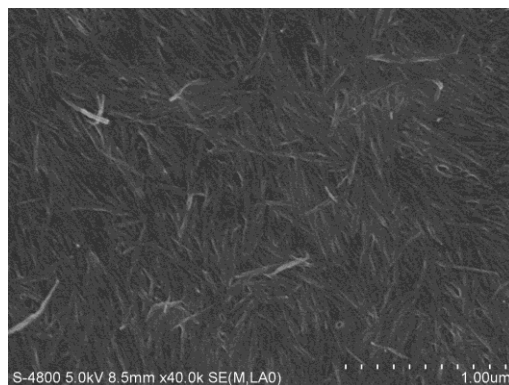


Fig. 1. FE-SEM micrograph of MCC

The combined treatment effectively disperses the MCC to rodlike whiskers, and some selected TEM micrographs for conditions 1, 2, 3, and 5, respectively, are given in Fig. 2. The CNWs from the combined treatments have a length of 199 to 344 nm, diameter of 11 to 33 nm, and aspect ratio of 10 to 18, as shown in Table 2, which shows that the materials possessed the intrinsic characteristic of CNWs (Beck-Candanedo *et al.* 2005; Siró and Plackett 2010).

Table 2. Size Distribution of Cellulose Nanowhiskers

Conditions	Diameter (nm)	Length (nm)	Aspect ratio
1	28	321	11
2	19	286	15
3	11	199	18
4	27	310	12
5	33	317	10
6	31	344	11
7	31	315	10

**Fig. 2.** TEM micrograph of CNWs with treatments (a) condition 1, (b) condition 2, (c) condition 3, and (d) condition 5**Fig. 3.** FE-SEM micrograph of CNWs treated with condition 3

With increasing sulfuric acid concentration from 20 to 60 wt%, CNWs decreased from 28 to 11 nm in diameter and 321 to 199 nm in length. The hydrolysis temperature and time slightly affected the size distribution of CNWs. Moreover, a uniform orientation is observed in Fig. 3 when using 60 wt% sulfuric acid; this also indicates a nematic liquid crystalline alignment (Orts *et al.* 1998; Beck-Candanedo *et al.* 2005).

Effects of Treatment on Chemical Components

Figure 4 shows the typical XPS survey spectra of MCC and CNWs obtained from conditions 1 and 3. An analysis of the survey spectra of MCC and CNWs indicated that the appearances of peaks at 532.0 eV and 286.0 eV were attributable to the presence of O(1s) and C(1s).

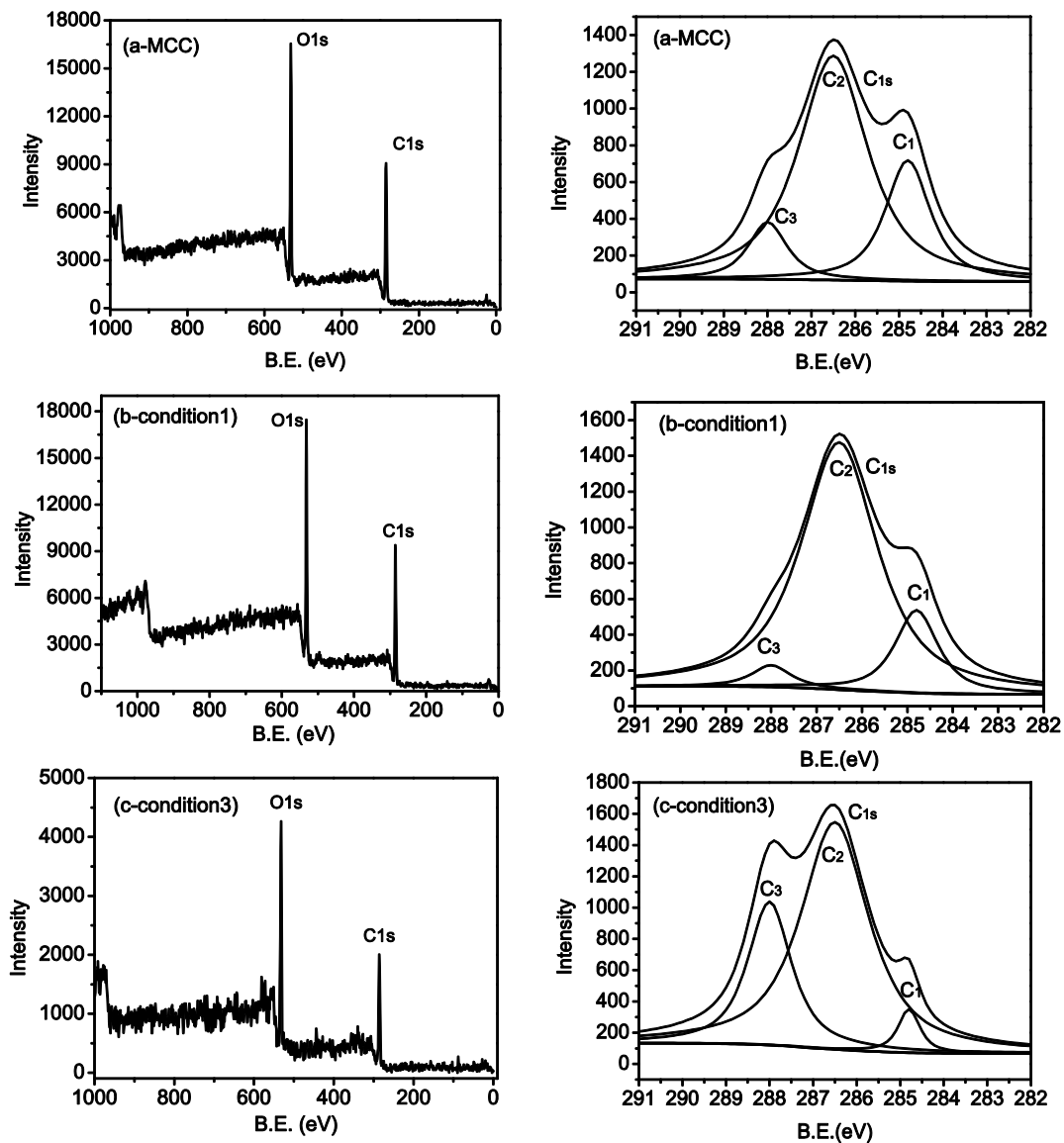


Fig. 4. C(1s) and O(1s) XPS survey spectra of (a) MCC, (b) CNWs from condition 1, and (c) CNWs from condition 3

The C(1s) signal is usually deconvoluted into four components according to the number of oxygen atoms bonded to C: (1) the C₁ class corresponds to carbon atoms bonded only with carbon or hydrogen atoms (C-C, C-H), (2) the C₂ class reveals the carbon atoms bonded with one oxygen atom (C-O, C-OH), (3) the C₃ class corresponds to carbon atoms bonded to a carbonyl or two non-carbonyl oxygen atoms (O-C-O, C=O), and (4) the C₄ class is associated with carbon atoms bonded to a carbonyl and a non-carbonyl oxygen atom (O=C-O) (Wistara *et al.* 1999; Inari *et al.* 2006). High resolution scans of the XPS spectra of C(1s) levels with their decomposition into four components are also presented in Fig. 4. Using the total areas of these peaks and the respective photoemission cross-sections, a quantitative determination of the O/C ratio could be calculated, and the results are shown in Table 3.

It is clear that the C₄ contributions (carboxyl bonding) had no effect on MCC and CNWs, and the contribution of the three types of carbons differed strongly between MCC and CNWs. Before combined treatment, three types of carbons were present in the structure of MCC with a greater contribution from the C₁ and C₂ classes and an O/C ratio of 0.60. With the combined treatment, CNWs reached a higher O/C ratio of 0.65 to 0.66, contributing to the hydrolysis of cellulose molecule during the combined treatment. With 20 wt% sulfuric acid, the C₁ contributions decreased from 23.5 to 15.4%, the C₂ contributions increased from 67.0 to 80.9%, and the C₃ contributions decreased from 9.5 to 3.7%. This is probably due to some breakages of intramolecular hydrogen bond and glycosidic bonds. With increasing sulfuric acid concentration up to 60 wt%, the C₁ contributions decreased gradually to 4.2%, while the C₂ contributions decreased to 68.1%, and the C₃ contributions (O-C-O, C=O) sharply increased to 27.6%. This could be due to the oxidation and interaction of micromolecules produced during hydrolysis of cellulose molecule at higher acid content in such a way that CNWs obtained a higher O/C ratio of 0.66.

Table 3. O/C Ratio and C₁, C₂, C₃, and C₄ Distribution of MCC and CNWs

Condition	O%	C%	O/C	C ₁ %	C ₂ %	C ₃ %	C ₄ %
MCC	37.47	62.53	0.60	23.5	67.0	9.5	0.0
1	39.41	60.69	0.65	15.4	80.9	3.7	0.0
3	39.86	60.14	0.66	4.2	68.1	27.6	0.0

FTIR Spectra Analysis

The FTIR spectra of MCC and CNWs are shown in Fig. 5, and the spectra are normalized at the peak of CH₂ (2900 cm⁻¹) in order to make comparisons between them. The strong absorptions nearly at 3420 cm⁻¹ are assigned to hydroxyl group stretching intramolecular hydrogen bonds (Dudley and Lan 1973; Chen *et al.* 2010). After nanofabrication, the intensity of these vibration peaks decreases due to some breakages of intramolecular hydrogen bonds. With increasing sulfuric acid concentration from 20 to 60 wt%, the breakages of intramolecular hydrogen bonds were exhibited more intensively, leading to a decrease in the intensity of the hydroxyl groups. In addition, two peaks at 1120, and 1060 cm⁻¹ are assigned to C-O vibration for MCC and CNWs, and the peaks at 900 cm⁻¹ are assigned to β-(1,4)-D-glycosidic bonds of cellulose (Gao and Tang 1996; Zhang *et al.* 2011). This is probably due to the breakage of glycosidic bonds after treatments, which is consistent with the XPS results.

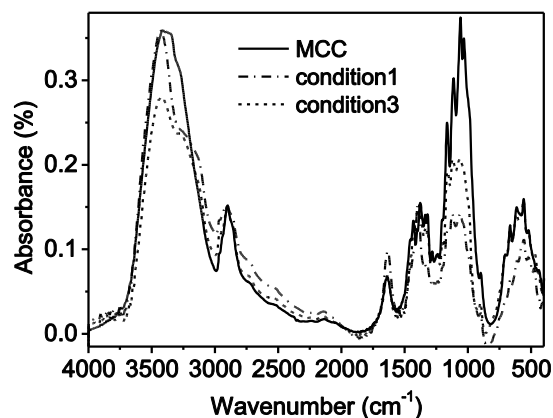


Fig. 5. FTIR spectra of MCC and CNWs

Effects of Treatment on Ultrastructure

The WAXD spectra of freeze-dried CNWs affected by treatments are shown in Fig. 6. The spectra of CNWs consist of crystalline peaks assigned to the (002) plane at $2\theta \approx 22.4\text{--}22.9^\circ$ and amorphous scatter at $2\theta \approx 18.2\text{--}19.2^\circ$ which represent typical cellulose I structure. The essential of cellulose crystals was not significantly changed by the treatments.

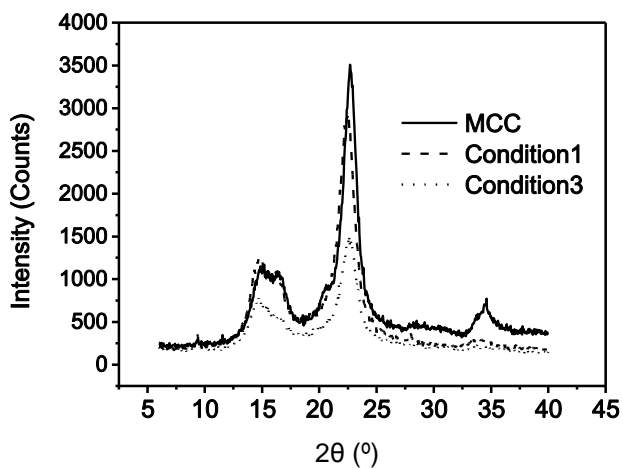


Fig. 6. The WAXD spectra of MCC and CNWs

The calculated crystallinity index of samples is given in Table 4. The crystallinity of CNWs was slightly lower than that of MCC. Before treatment, MCC had a higher crystallinity index of 92.4%. After the combined treatments, CNWs had a decreased crystallinity index of 82.5 to 89.8%. CNWs treated with 60 wt% sulfuric acid (condition 3) had a lower crystallinity index of 82.5%. In contrast to the cellulose nanocrystals with higher crystallinity after hydrolysis (Hamad and Hu 2010; Li *et al.* 2011), the crystallinity of the CNWs was slightly lower than that of MCC in this work. This observation means that the hydrolysis reaction not only occurred at the amorphous region of MCC but also occurred at their crystalline region (Wang *et al.* 2008), or else the CNWs should have a higher crystallinity than that of MCC.

Table 4. Crystallinity index of MCC and CNWs (%)

Conditions	<i>Crl</i>
MCC	92.4 (0.40) ^a
1	88.4 (1.05)
2	89.8 (0.88)
3	82.5 (5.54)
5	90.7 (1.48)
6	89.7 (1.39)
7	88.0 (1.98)
Straw fiber ^b	63.4 (3.68)

a: Values in parentheses are the standard deviations of the two measurements.

b: Pan *et al.* (2010)

CONCLUSIONS

Cellulose nanowhiskers were prepared with a combination of acid hydrolysis and high pressure homogenization, and surface morphology and chemical properties of the obtained nanowhiskers were investigated. After the combined treatment, nanoparticles were produced that exhibit rodlike whiskers with a diameter of 11 to 33 nm, a length of 199 to 344 nm, and aspect ratio of 10 to 18, corresponding to the intrinsic characteristic of cellulose nanowhiskers. The FTIR and XPS results show that some breakages of intramolecular hydrogen bond and glycosidic bonds occurred during the hydrolysis reaction of MCC. An increase in acid concentration from 20 to 60 wt% could accelerate these breakages in the cellulose molecule, leading to effective production of narrower, less poly-disperse nanowhiskers with lower crystallinity.

ACKNOWLEDGMENTS

This study was supported by a Foundation for the Author of National Excellent Doctoral Dissertation of PR China (FANEDD, Grant No. 201173) and the Key (Keygrant) Project of Chinese Ministry of Education (Grant No. 212064). The authors would like to thank Wengang Yu and Juhua Jiang for their technical assistance.

REFERENCES CITED

- Bai, W., Holbery, J., and Li, K. C. (2009). "A technique for production of nanocrystalline cellulose with a narrow size distribution," *Cellulose*. 16, 455-465.
- Beck-Candanedo, S., Roman, M., and Gray, D. G. (2005). "Effect of reaction conditions on the properties and behavior of wood cellulose nanocrystal suspensions," *Biomacromolecules* 6, 1048-1054.
- Bondeson, D., Mathew, A., and Oksman, K. (2006). "Optimization of the isolation of nanocrystals from microcrystalline cellulose by acid hydrolysis," *Cellulose*. 13, 171-180.

- Chen, W. S., Yu, H. P., Liu, Y. X., Jiang, N. X., and Chen, P. (2010). "A method for isolating cellulose nanofibrils from wood and their morphological characteristics," *Acta. Polym. Sin.* 11, 1320-1326.
- Dong, X. M., Revol, J. F., and Gray, D. G. (1998). "Effect of microcrystallite preparation conditions on the formation of colloid crystals of cellulose," *Cellulose.* 5, 19-32.
- Dudley, H. W., and Lan, F. (1973). *Spectroscopic Methods in Organic Chemistry*, 2nd Edn., McGraw-Hill. London, New York.
- Elazzouzi-Hafraoui, S., Nishiyama, Y., Putaux, J. L., Heux, L., Dubreuil, F., and Rochas, C. (2008). "The shape and size distribution of crystalline nanoparticles prepared by acid hydrolysis of native cellulose," *Biomacromolecules* 9, 57-65.
- El-Sakhawy, M., and Hassan, M. L. (2007). "Physical and mechanical properties of microcrystalline cellulose prepared from agricultural residues," *Carbohyd. Polym.* 67(1), 1-10.
- Fan, J. S., and Li, Y. H. (2012). "Maximizing the yield of nanocrystalline cellulose from cotton pulp fiber," *Carbohyd. Polym.* 88(4), 1184-1188.
- Favier, V., Chanzy, H., and Cavaille, J. Y. (1995). "Polymer nanocomposites reinforced by cellulose whiskers," *Macromolecules.* 28, 6365-6367.
- Gao, J., and Tang, L. G. (1996). *Cellulose Science*, Science Press, Beijing.
- Gray, D. G. (2008). "Transcrystallization of polypropylene at cellulose nanocrystal surfaces," *Cellulose* 15, 297-301.
- Hamad, W. Y., and Hu, T. Q. (2010). "Structure-process-yield interrelations in nanocrystalline cellulose extraction," *Can. J. Chem. Eng.* 88, 392-402.
- Helbert, W., Cavaille, J., and Dufresne, A. Y. (1996). "Thermoplastic nanocomposites filled with wheat straw cellulose whiskers. Part I. Processing and mechanical behavior," *Polym. Composite.* 17, 604-611.
- Inari, G. N., Petrissans, M., Lambert, J., Ehrhardt, J. J., and Gérardin, P. (2006). "XPS characterization of wood chemical composition after heat-treatment," *Surf. Interface. Anal.* 38, 1336-1342.
- Kulkarni, A., and Mahanwar, P. A. (2011). "Effect of dispersion of nanofibers on the properties of LDPE Films," *Int. J. Plast. Technol.* 15, 77-85.
- Leitner, J., Hinterstoisser, B., Wastyn, M., Keckes, J., and Gindl, W. (2007). "Sugar beet cellulose nanofibril-reinforced composites," *Cellulose.* 14, 419-425.
- Li, W., Wang, R., and Liu, S. (2011). "Nanocrystalline cellulose prepared from softwood kraft pulp via ultrasonic-assisted acid hydrolysis," *BioResources* 6(4), 4271-4281.
- Liu, H. Y., Liu, D. G., Yao, F., and Wu, Q. L. (2010). "Fabrication and properties of transparent polymethylmethacrylate/cellulose nanocrystals composites," *Bioresource. Technol.* 101, 5685-5692.
- Martínez-Sanz, M., Lopez-Rubio, A., and Lagaron, J. M. (2011). "Optimization of the nanofabrication by acid hydrolysis of bacterial cellulose nanowhiskers," *Carbohyd. Polym.* 85, 228-236.
- Oksman, K., Mathew, A. P., Bondeson, D., and Kvien, I. (2006). "Manufacturing process of cellulose whiskers/polylactic acid nanocomposites," *Compos. Sci. Technol.* 66, 2776-2784.
- Oksman, K., Mathew, A. P., and Sain, M. (2009). "Novel bionanocomposites: processing, properties and potential applications," *Plast. Rubber. Compos.* 38, 396-405.

- Orts, W. J., Godbout, L., Marchessault, R. H., and Revol, J. F. (1998). "Enhanced ordering of liquid crystalline suspensions of cellulose microfibrils: A small angle neutron scattering study," *Macromolecules*. 31, 5717-5725.
- Pan, M. Z., Zhou, D. G., Zhou, X. Y., and Lian, Z. N. (2010). "Improvement of straw surface characteristics via thermomechanical and chemical treatments," *Bioresour. Technol.* 101, 7930-7934.
- Sadeghifar, H., Filpponen, I., Clarke, S. P., Brougham, D. F., and Argyropoulos, D. S. (2011). "Production of cellulose nanocrystals using hydrobromic acid and click reactions on their surface," *J. Mater. Sci.* 46, 7344-7355.
- Samir, M., Alloin, F., and Dufresne, A. (2005). "Review of recent research into cellulosic whiskers, their properties and their application in nanocomposite field," *Biomacromolecules* 6(2), 612-626.
- Samir, M., Alloin, F., Sanchez, J. Y., El Kissi, N., and Dufresne, A. (2004). "Preparation of cellulose whiskers reinforced nanocomposites from an organic medium suspension," *Macromolecules* 7, 1386-1393.
- Siqueira, G., Bras, J., and Dufresne, A. (2010). "Cellulosic bionanocomposites: A review of preparation, properties and applications," *Polymers*. 2, 728-865.
- Siró, I., and Plackett, D. (2010). "Microfibrillated cellulose and new nanocomposite materials: a review," *Cellulose*. 17(3), 459-494.
- Wang, N., Ding, E., and Cheng, R. (2008). "Preparation and liquid crystalline properties of spherical cellulose nanocrystals," *Langmuir*. 24, 5-8.
- Wang, Q. Q., Zhu, J. Y., Reiner, R. S., Verrill, S. P., Baxa, U., and McNeil, S. E. (2012). "Approaching zero cellulose loss in cellulose nanocrystal (CNC) production: recovery and characterization of cellulosic solid residues (CSR) and CNC," *Cellulose* 19, 2033-2047.
- Wistara, N., Zhang, X. J., and Young, R. A. (1999). "Properties and treatments of pulps from recycled paper. Part II. Surface properties and crystallinity of fibers and fines," *Cellulose* 6, 325-348.
- Zhang, L. P., Tang, H. W., Qu, P., Li, S., Qin, Z., and Sun, S. Q. (2011). "Spectral property of one dimensional rodlike nano cellulose," *Spectroscopy. Spectral. Analysis* 31, 1097-1100.
- Zhou, C. J., Wu, Q. L., Yue, Y. Y., and Zhang, Q. G. (2011). "Application of rod-shaped cellulose nanocrystals in polyacrylamide hydrogels," *J. Colloid. Interf. Sci.* 353, 116-123.

Article submitted: October 8, 2012; Peer review completed: December 8, 2012; Revised version received and accepted: January 6, 2013; Published: January 7, 2013.